Earth and Planetary Science Letters 375 (2013) 209–221

Contents lists available at ScienceDirect

Earth and Planetary Science Letters

journal homepage: www.elsevier.com/locate/epsl

# Cyclical patterns in volcanic degassing revealed by $SO_2$ flux timeseries analysis: An application to Soufrière Hills Volcano, Montserrat ☆

E.J. Nicholson [a,b,*], T.A. Mather [a], D.M. Pyle [a], H.M. Odbert [b,c], T. Christopher [c]

[a] Department of Earth Sciences, University of Oxford, South Parks Road, Oxford OX1 3AN, UK
[b] Department of Earth Sciences, University of Bristol, Wills Memorial Building, Bristol BS8 1RJ, UK
[c] Montserrat Volcano Observatory, Montserrat, West Indies

ARTICLE INFO

*Article history:*
Received 11 October 2012
Received in revised form
10 May 2013
Accepted 20 May 2013
Editor: T. Elliot
Available online 4 July 2013

*Keywords:*
timeseries analysis
degassing
lava dome
periodic behaviour

ABSTRACT

Cyclical patterns of behaviour in timeseries of seismic and geodetic data at volcanoes are frequently observed during lava dome-building eruptions, and are particularly well-documented from the current eruption of the Soufrière Hills Volcano (SHV), Montserrat. However, the discontinuous nature of many $SO_2$ measurements often preclude the identification and quantitative analysis of cyclical patterns in degassing data. Here, using a long $SO_2$ timeseries from SHV, with continuous measurements since 2002, we explore for the first time degassing behaviour at a resolution comparable to that possible for seismic and deformation datasets. Timeseries analysis of flux data spanning 2002–2011 reveals that $SO_2$ emissions at SHV exhibit complex cyclicity, with dominant cycles evident on both multi-year and multi-week (~50 day) timescales. These cycles persist through phases of both active extrusion and eruptive pause, and show close similarities to periodic components previously identified at SHV in timeseries of seismicity, ground deformation and lava extrusion.

The strength of expression or amplitude of degassing cycles, particularly on multi-week timescales, shows distinct temporal variation, and appears to correlate with the occurrence and nature of explosive activity occurring in 2002–2009. This suggests that the amplitude of surface gas flux cycles is modulated by physical conditions within the conduit. Direct quantitative comparison between seismicity, dome growth, and degassing for eruptive Phases 2 (2002–2003) and 3 (2005–2007) reveals that peaks in $SO_2$ flux appear to correspond broadly to enhanced lava extrusion and elevated seismicity within cycles of 30–50 days. However, time lags of 2, 4 and 7 days are observed between initial low-frequency seismic swarms and peaks in dome growth, $SO_2$ flux and rockfall event rate respectively. Multi-parameter correlations offer valuable insights into the controls on subsurface gas ascent, but further research is required to fully explore the contributions of permeability and overpressure, as well as other subsurface processes.



## 1. Introduction

Long-lived dome-forming eruptions are common features of andesitic volcanoes in subduction-zone settings (e.g., Newhall and Melson, 1983; Sparks, 1997). Activity is characterised by the extrusion of viscous, degassed, and often crystal-rich magma, which typically accumulates close to the vent and can build complex edifices ranging up to several cubic kilometres in volume. Dome-forming eruptions engender significant local hazards, because of the potential for catastrophic collapse, and the propensity for these systems to switch between effusive and explosive phases of activity (e.g., Matthews et al., 1997; Sparks and Aspinall, 2004; Voight et al., 1999).

The periodic behaviour of a number of parameters has been documented during many dome-forming eruptions, and probably reflects the fundamental eruptive mechanisms occurring at these volcanic systems during eruption. Cycles can either remain stable, or show systematic or non-systematic temporal changes (Denlinger and Hoblitt, 1999). Cycles in multiple physical observables, including lava efflux, seismic energy and event rate, ground deformation and degassing, have been observed at Mt St Helens (USA; Swanson and Holcomb, 1990), Santiaguito (Guatemala; Harris et al., 2003; Holland et al., 2011; Sahetapy-Engel et al., 2004) and Soufrière Hills Volcano (Montserrat; Edmonds et al., 2003a;



* Corresponding author at: Department of Earth Sciences, University of Bristol, Wills Memorial Building, Bristol BS8 1RJ, UK.
*E-mail address:* en12525@bristol.ac.uk (E.J. Nicholson).

0012-821X 
http://dx.doi.org/10.1016/j.epsl.2013.05.032

Loughlin et al., 2010; Voight et al., 1999, 1998; Wadge et al., 2010; Watson et al., 2000; Young et al., 1998) among others (Table A; Supplementary information). Recent advances in geophysical monitoring have allowed systematic behaviour to be studied at increasingly fine time resolution. Nevertheless, much of the previous work in this field has focussed on single parameters (e.g., tilt deformation; Anderson et al., 2010; Voight et al., 1998), and less work has been done to analyse quantitatively the rich information contained within the multi-parameter geophysical and geochemical datasets that are increasingly common at well-monitored volcanoes (e.g., Aiuppa et al., 2010; Bonaccorso et al., 2011; Landi et al., 2011).

While spectral analysis is a well-developed tool for timeseries analysis in other parts of geosciences (e.g., climatology; Ghil et al., 2002; Mann and Lees, 1996) quantitative spectral analysis has only recently been applied in volcanology (Odbert and Wadge, 2009; Pearson et al., 2008). Here, we show how timeseries analysis techniques can be used to quantify the cyclical patterns of $SO_2$ flux at volcanic systems with long records of degassing data, and how quantitative analysis of long-term geophysical monitoring datasets can be used to reveal new insights into the behaviour of the volcanic system. Specifically, we use $SO_2$ flux timeseries data from Soufrière Hills Volcano (Fig. 1) to explore for the first time degassing trends at a resolution comparable to other geophysical parameters. Periodicities in $SO_2$ flux, and their temporal variability, are quantified and compared with characteristic timescales observed in other geophysical parameters in order to gain insights into the processes influencing shallow gas ascent.

### 1.1. Soufrière Hills Volcano, Montserrat

The current eruption at Soufrière Hills Volcano (SHV) began in 1995, and has been exceptionally well documented during both the early eruptive phases (e.g., Druitt and Kokelaar, 2002; Watts et al., 2002; Young et al., 1998), and as in more recent long-term overviews (Christopher et al., 2010; Luckett et al., 2007; Wadge et al., 2010). Activity is very broadly characterised by 2–3 yr ('multi-year') phases of active dome growth, separated by eruptive pauses (Fig. 1). Rapid transitions between effusive and explosive behaviour have been observed during some phases (e.g., Melnik and Sparks, 1999, 2005). During several extended periods of discrete explosions, for example, the explosive events are often correlated with cyclicity in other parameters, providing the potential for forecasting during these periods of quasi-systematic behaviour and evidence for links with conduit processes (Connor et al., 2003; Jaquet et al., 2006; Pyle, 1998; Watt et al., 2007). A series of Vulcanian explosions occurred at SHV in July 1997, each preceded by swarms of long-period seismicity and coincident with tilt cycle maxima (Voight et al., 1998). Similar behaviour has also been observed throughout later phases of the eruption, most notably in 2008–2010 (Odbert et al., in press). Studies integrating multiple parameters can therefore potentially provide significant insights into the mechanisms governing periodic behaviour.

Previous studies of the cyclicity observed in tiltmeter deformation and seismic events/amplitude timeseries at SHV have revealed both sub-daily (~8 h) and multi-week (6–8 week or '50-day') timescales (Loughlin et al., 2010; Odbert and Wadge, 2009; Voight et al., 1998). Recent numerical models have shown these cycles to be mutually coupled, whereby variation in one cycle influences the amplitude and/or frequency of the other (Costa et al., 2013). Cyclical behaviour is often the result of multiple competing processes, with periodic stick-slip magma plug motion, in response to pressurisation in the shallow conduit, generally invoked to explain the sub-daily cycles (Costa et al., 2012, 2013; Denlinger and Hoblitt, 1999; Lensky et al., 2008; Thomas and Neuberg, 2012; Voight et al., 1999).

The numerical model of Costa et al. (2007a,b, 2013) represents the only attempt made thus far to model the longer multi-week cycles, and attributes cyclicity to feedbacks between magma ascent, seismicity and ground deformation associated with the periodic expansion and contraction of an elastic lower conduit dyke. The model produces a modulation of the magma flow into the shallow conduit over timescales of ~50-days, driven by the periodic development and release of overpressure at dyke depths of 2–5 km. Higher amplitude tilt cycles, combined with overall deflation, and enhanced low-frequency (LF) seismicity occur during periods with elevated magma ascent rates early in each multi-week cycle (Costa et al., 2007a,b, 2013; Voight et al., 1999). Nevertheless, the implications of this model for degassing have only been addressed qualitatively. Initial attempts to link geophysical and degassing cycles were hindered by the challenges of regularly sampling $SO_2$ fluxes early in the eruption (e.g., Watson et al., 2000; Young et al., 2003). The installation of an automated network of UV-spectrometers in 2002 permitted collection of a

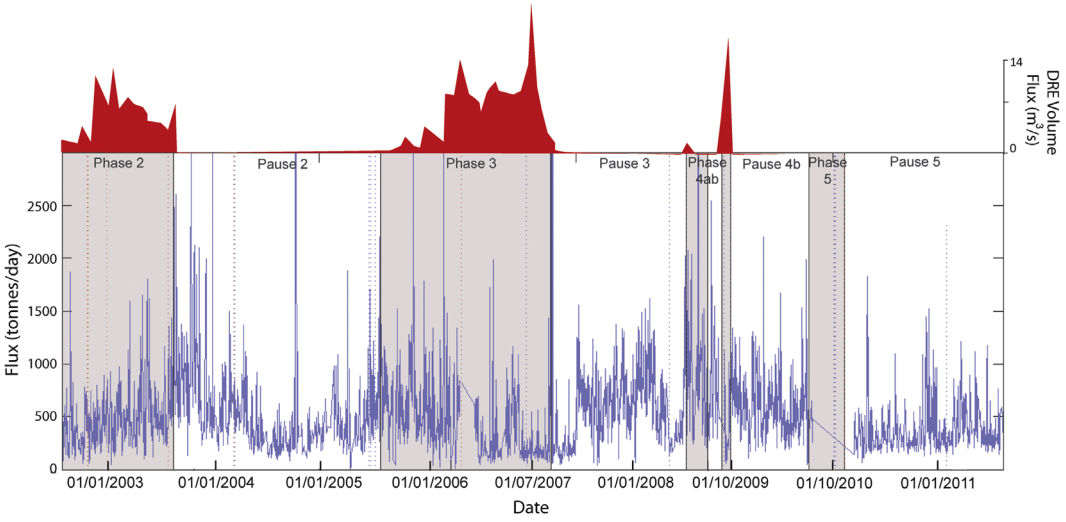


**Fig. 1.** Timeseries of daily mean $SO_2$ flux since the onset of continuous daily sampling (2002–2011) acquired by MVO using the instrumentation and methodology detailed in Edmonds et al. (2003b). Periods of active dome growth are annotated and highlighted (shaded regions) with the variable rates of magma efflux shown at the top in red in units of dense rock equivalent (DRE) volume (2002–2009; Wadge et al., 2010). (For interpretation of the references to colour in this figure legend, the reader is referred to the web version of this article.)

continuous, regularly-sampled dataset (Fig. 1; Edmonds et al., 2003b), which is now long enough for robust analysis.

Patterns of $SO_2$ degassing at SHV are complex, and cannot be reconciled with closed-system degassing of a single batch of magma (Edmonds et al., 2003a). Surface flux is highly variable on a range of timescales (Edmonds et al., 2003a; Young et al., 1998). $SO_2$ is believed to originate from the volcano's deep magma supply, which is generally assumed to be supplied at a constant rate of 1–2 $m^3\,s^{-1}$ (e.g., Foroozan et al., 2011); therefore, the measured variable degassing rates likely reflect concurrent changes in shallow gas ascent (Edmonds et al., 2001, 2003a,b). Long-term degassing trends appear independent of magma extrusion phases (Fig. 1; Edmonds et al., 2010), implying the development of sufficient permeability to allow gas transport to the surface from magma chamber depths even during pauses in extrusive activity.

## 2. Data acquisition and methodology

$SO_2$ flux has been measured continuously at SHV since 2002 by a network of fixed scanning UV-DOAS spectrometers. $SO_2$ absorption spectra are collected between 07:00 and 17:00 each day. Flux estimates are derived by multiplying the integrated plume concentration for each scan spectrum by the width and speed of the plume (Edmonds et al., 2003b). The timeseries of daily average flux used in this study (2631 measurements over 3347 days from 2002–2011) is shown in Fig. 1. Linear interpolation has been applied over data gaps spanning fewer than 14 values. A prolonged data hiatus between October 2009 and March 2010 precludes analysis of data windows during this period.

### 2.1. Timeseries analysis methods

Timeseries analysis can be used to quantify cyclic behaviour in geophysical systems. In this study, we evaluate data in both the time and frequency domains to explore the different properties of the timeseries.

#### 2.1.1. Spectral analysis

Volcanic systems are inherently non-linear, and can exhibit strongly periodic behaviour on a variety of timescales (Barmin et al., 2002; Denlinger and Hoblitt, 1999; Melnik and Sparks, 1999, 2005). The signals of multiple, superposed cycles from a dataset can be deconvolved by Fast Fourier Transform (FFT) analysis, to reveal the frequency, and relative importance, of underlying periodic components. The end product of spectral analysis is an estimate of the Power Spectral Density (PSD, Percival and Walden, 1993), and this can be displayed graphically to highlight the frequency intervals over which cyclicity is most strongly manifest for the dataset of interest (e.g., Fig. 2).

The spectral analyses performed for this study were calculated using the SSA-MTM Toolkit presented in Ghil et al. (2002). Data were prepared for analysis using a detrending correction to render the timeseries approximately stationary (as required for the algorithm), then either padded with zeroes at either end or truncated to a length of $n^2$ samples, for integer $n$, as required for FFT. The Multitaper Method (MTM) is adopted in this study as it provides the most robust PSD estimation when there is no prior knowledge of the signal-generating source (Thomson, 1982). The significance of peaks in MTM spectra are assessed against a statistical red noise model (RNM; Mann and Lees, 1996), the use of which is appropriate for geophysical systems when it is often the case that processes acting over timescales greater than the selected sample lengths exert a strong control on the nature of the background noise. Without knowledge of the noise-generating sources, however, it is impossible to fully characterise the nature of the noise. Therefore, the RNM applied here is intended to guide interpretation, rather than to provide a rigorous statistical test.

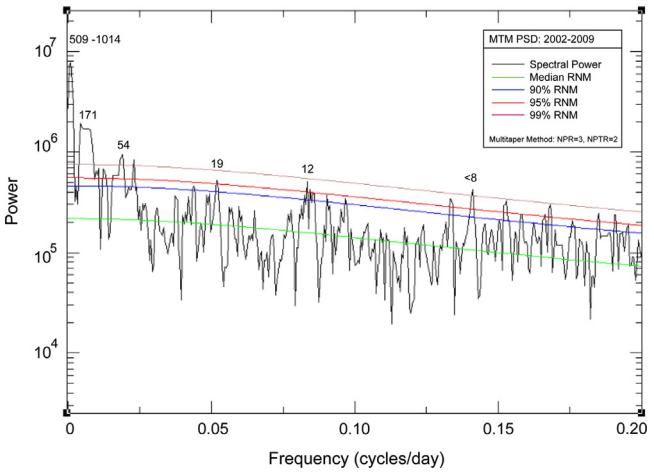


**Fig. 2.** Multitaper spectrum showing 2002–2009 power spectral density (PSD) estimate for the first 2028 values of the $SO_2$ flux timeseries for frequencies up to 0.2 cycles/day (start date—1 July 2002). The central peaks exceeding at least the 90% confidence red noise model (RNM) are annotated with the corresponding cycle periods (days). The lines in the figure and figure legend are in colour. To view these in colour the reader is referred to the web version of this article.

#### 2.1.2. Reconstructive analysis

Reconstructive analysis was performed to provide an internal check that the MTM results presented in Section 3.1 indeed represent the $SO_2$ timeseries. This technique tests the hypothesis that the raw dataset can be approximated by a composite sine wave composed of its dominant periodicities (Eq. (1)); a similar concept was introduced by Ghil et al. (2002) for the reconstruction of climatic records.

Reconstructions assigning equal significance to each cycle offer an insufficient match to the raw data, so the final composite wave is weighted according to relative confidence levels attributed to each component (Table 1):

$$\textit{reconstructed flux},\ q = A\sin\left(\frac{2\pi f_1 t}{f_s}\right) + B\sin\left(\frac{2\pi f_2 t}{f_s}\right) + C\sin\left(\frac{2\pi f_3 t}{f_s}\right) \qquad (1)$$

where $f_s$ is the sampling frequency (i.e. daily), $t$ is the length of the dataset (approximately 512–1024 datapoints), $f_{1-3}$ is the frequencies corresponding to cycle periods identified by MTM analysis (Table 1). $A$, $B$ and $C$ are optimal weighting coefficients determined by least-squares regression of the model to the raw timeseries.

#### 2.1.3. Short-term Fourier Transform (STFT)

Statistical stationarity, required over the complete data window for MTM analysis, may not strictly be achieved in many geophysical systems known to exhibit temporal evolution in cyclic behaviour even after a detrending correction, thus resulting in broad undefined peaks in frequency spectra that are difficult to interpret. The Short-term Fourier Transform (STFT) calculates a series of PSD estimates using a moving window of specified length, and displays them as a composite spectrogram (Odbert and Wadge, 2009). The reduced window length used to generate these spectrograms will not only minimise the influence of any non-stationary behaviour remaining in the timeseries after detrending corrections, but also enable any temporal variation in the frequency distribution to be explored.

The choice of both window length and overlap is critical to the analysis, and has been optimised for each analysis depending on the cycles of interest (see sensitivity study in Supplementary methods). Window lengths of 256–128 days (with overlaps ranging from 50% to 99%) were found to provide the best compromise between achieving

**Table 1**
Complete results of Multitaper analysis.

| Analysis interval (number of samples) | Peak frequency (cycles/day) | Peak distribution (cycles/day) | Confidence level (%) | Cycle peak period (days) | Cycle period range (days) |
|---|---|---|---|---|---|
| 2002–2009 (2028) | 0.00196 | 0.000986–0.00196 | 99 | 1014 | 509–1-14 |
| | 0.0185 | 0.0159–0.0244 | 99 | 54 | 41–63 |
| | 0.0526 | 0.0370–0.0588 | 95 | 19 | 12–27 |
| | 0.0833 | 0.0759–0.100 | 95 | 12 | 10–13 |
| | 0.125 | > 0.125 | 99 | 8 | < 8 |
| Phase 2 (512) | 0.0244 | 0.0238–0.0278 | 90 | 41 | 36–42 |
| | 0.0385 | 0.0357–0.0400 | 95 | 26 | 25–28 |
| | 0.0667 | 0.0625–0.0667 | 90 | 15 | 15–16 |
| | 0.167 | > 8 | 99 | 6 | < 6 |
| Pause 2 (512) | 0.0244 | 0.0137–0.0270 | 95 | 53 | 37–73 |
| | 0.0385 | 0.03570.0400 | 90 | 26 | 25–28 |
| | 0.0588 | 0.0588 | 90 | 17 | 17 |
| | 0.0909 | 0.0909–0.100 | 99 | 11 | 10–11 |
| | 0.167 | > 0.167 | 90 | 6 | < 6 |
| Phase 3 (512) | 0.0192 | 0.0137–0.0204 | 99 | 52 | 49–73 |
| | 0.0909 | 0.0833–0.0909 | 95 | 11 | 11–12 |
| | 0.125 | > 0.125 | 90 | 8 | < 8 |
| Pause 3 (512) | 0.0222 | 0.0164–0.0204 | 99 | 45 | 43–61 |
| | 0.0526 | 0.0500–0.0556 | 90 | 19 | 18–20 |
| | 0.0909 | 0.0909 | 90 | 11 | 11 |
| | 0.0200 | > 0.0200 | 95 | 5 | < 5 |
| Pause 4b (256) | 0.0714 | 0.0667–0.0769 | 95 | 14 | 13–15 |
| | 0.167 | > 6 | 95 | 6 | < 6 |
| Pause 5 (512) | 0.0400 | 0.0303–0.0400 | 95 | 25 | 25–33 |
| | 0.0667 | 0.0625–0.0714 | 95 | 15 | 14–16 |
| | 0.909 | 0.909–0.100 | 99 | 11 | 10–11 |

sufficient temporal resolution and maintaining a long enough window for robust analysis. Each PSD estimate has also been normalised to unity to remove the influence of changes in the absolute spectral power, thereby allowing direct comparison of the relative frequency distributions between contiguous windows.

#### 2.1.4. Cross-correlation analysis

If an association exists between two parameters, but the response is delayed in time, then a simple correlation between aligned sequences is inadequate to capture the relationship. Cross-correlation explores the relationship between two timeseries shifted relative to one another as a function of time (Percival and Walden, 1993). At each lag (i.e., multiples of the daily sampling interval) the integrated product of the two timeseries ($x$ and $y$) is calculated and the correlation coefficient, $\varphi$, determined (Eq. (2)).

$$\text{correlation coefficient } \varphi = \frac{\sum[x(i)-mean(x)] \times [y(i-lag)-mean(y)]}{\sqrt{\sum[x(i)-mean(x)]^2} \times \sqrt{\sum[y(i-lag)-mean(y)]^2}} \quad (2)$$

A similar method was applied in Matthews et al. (2009) to explore the link between rainfall events and seismicity at SHV over hourly timescales. The relatively low signal-to-noise ratio in the $SO_2$ timeseries means that patterns in the relative correlation ($\varphi$) are more relevant than the absolute value.

## 3. Results

### 3.1. Multitaper Method (MTM) results

The complete results of MTM analysis are displayed in Table 1, including analyses of both the complete timeseries and individual eruptive phases (eruption chronology in Fig. 1), and summarised in Table 2. The Power Spectral Density (PSD) estimate for the complete timeseries (1 July 2002–9 October 2009) is displayed in Fig. 2 (see Supplementary information for PSD spectra for each eruptive phase).

**Table 2**
Summary of spectral analysis results: cycles are described by their central period (days) and classified based on the level of confidence at which this peak exceeds the Red Noise Model (RNM).

| Analysis interval | 99% confidence | 95% confidence | 90% confidence |
|---|---|---|---|
| 2002–2009 | 509–1014 | 19 | |
| | 54[a] | 12[b] | |
| | 8 | | |
| Phase 2 (01/08/02–31/07/03) | 6 | 26 | 41[a] |
| | | | 14[b] |
| Pause 2 (01/08/03–07/08/05) | 11[b] | 53[a] | 17 |
| | | | 26 |
| | | | 6 |
| Phase 3 (08/08/05–03/04/07) | 52[a] | 11[b] | 8 |
| Pause 3 (04/04/07–28/07/08) | 45[a] | 5 | 11[b] |
| | | | 19 |
| Pause 4b (04/01/09–08/10/09) | | 14[b] | |
| | | 6 | |
| Pause 5 (01/03/10–29/08/11) | 11[b] | 25 | |
| | | 15 | |

[a] These periods are in the range 41–63 days and are interpreted to represent a single characteristic periodicity of the system (referred to as the '50-day cycle').
[b] These periods are in the range 10–14 days and are interpreted to represent a second characteristic periodicity of the system.

### 3.1.1. 2002–2009

The analysis shows that the PSD distribution is consistent with that of multiple periodic components superimposed on background noise (well described by the red noise model; RNM). Several peaks of variable width and amplitude are significant above noise confidence thresholds. Three dominant peaks lying towards the low-frequency end of the spectrum, with cycle periods of 509–1014, 171, and 54 days, have 99% significance. However, 171 days has been highlighted during the analysis as a probable harmonic feature by the reshaping procedure described in Ghil et al. (2002). Peak widths vary between each cyclic component, reflecting their different power distributions. Broader peaks centred on periods of 19 and 12 days are significant above 95%, but not 99%, confidence levels. The lower relative power amplitude of these cycles compared to the longer cycles is a result of the greater range of frequencies over which their spectral power is distributed. Broad peaks often indicate temporal variation in cycle frequency, implying that these weaker cycles are either unstable or a possible artefact of the methodology; cyclicity on these timescales is also not strongly detected in either STFT (Section 3.3) or cross-correlation analyses (Section 3.4). Sustained high power is also apparent at periods $<8$ days.

Analyses of each eruptive phase (Table 1; Fig. B, Supplementary information) support the observations from the 2002–2009 power spectrum (Fig. 2). Cyclic behaviour is evident on a variety of timescales, many components of which persist through all phases. These components can be grouped into long-, mid-, and short-term cycles, with periods of 509–1014 days, 41–63 days, 17–26/11–14 days respectively (highlighted in Table 2). The 41–63 day periodicity (hereafter referred to as the multi-week cycle) is strongly significant relative to the noise model at the 99% confidence level in the analysis of the complete timeseries, and is often the most well-defined spectral peak in analyses of those sub-sections spanning a time interval sufficient to robustly detect cyclicity on this timescale (Fig. 2; Fig. B, Supplementary information). The multi-week cycle therefore appears to dominate the $SO_2$ flux. Higher-frequency variation on timescales $<8$ days may be significant, but the large uncertainties in flux measurements (Edmonds et al., 2003b) mean these components should be interpreted with caution. The daily sampling of the $SO_2$ flux dataset is insufficient to resolve cyclicity on timescales $<2$ days.

Slight frequency variation for all peaks (corresponding to variance in cycle period over several days), identified by the broad nature of the peaks in the 2002–2009 spectrum (Fig. 2), has been confirmed by comparing the frequency distributions of individual phases (Supplementary information), which show peaks at similar frequencies but with slight discrepancies of 0.02–0.03 cycles/day. This is not unexpected in a physical system governed by complex interactions between multiple processes and feedbacks operating on several timescales. The broad consistency in the spectral characteristics of both periods of active extrusion and repose is surprising, given the substantial change in eruptive behaviour. This result is consistent, however, with the observation that the long-term trends in $SO_2$ flux (identified both visually in Fig. 1 and quantitatively by MTM analysis) appear to be independent of the eruptive state of the volcano (i.e., paused or active dome growth; Christopher et al., 2010; Edmonds et al., 2003a, 2010).

## 3.2. Reconstructive analysis results

Reconstructive analysis was applied initially to the Phase 3 dataset (Fig. 3), for which the broad spectral peaks in the MTM spectrum most strongly suggested cycle instability (Fig. B, Supplementary information), to test the validity of the MTM results. The optimum weighting configuration, determined by least squares regression of the multiple reconstructions to the raw timeseries, was found to favour the 52-day component (Table 1), suggesting that processes governing cyclicity on this time-scale dominated the system during this phase.

The reconstructed timeseries correlates well with the raw data prior to the dome collapse event (20 May 2006), but fails to provide such a good representation subsequently. Applying a lag offset of 25–30 days to the 52-day component, in addition to slight lengthening of the cycle period, brings the reconstructed timeseries back into correlation with the raw data, but, even then, the agreement is less convincing. This may point to a fundamental change in $SO_2$ degassing following a large-scale dome collapse.

Reconstructive analysis was repeated for each of the MTM analyses described in Section 3.1 (Fig. C, Supplementary information). Although, in general, the reconstructed timeseries provide a reasonable match to the raw data, it is apparent that the strength of the fit varies temporally. An offset applied to the reconstruction, or a slight change in the cycle period, is often required to provide the best visual match to different sections of the data, implying phase shifts in the system's cyclic behaviour. The transitions appear abrupt, rather than gradational, and are often associated

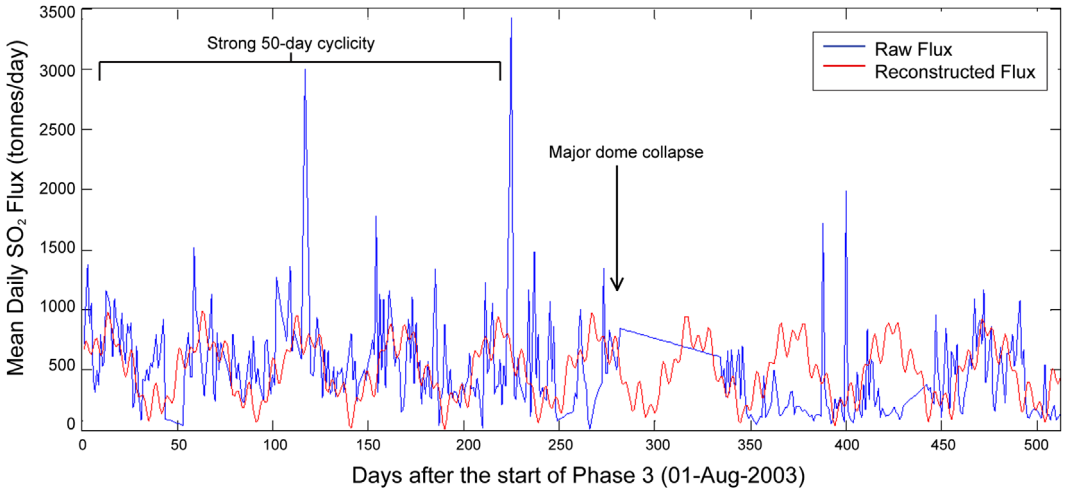


**Fig. 3.** Reconstruction of eruptive Phase 3: comparison of reconstructed flux (shown in red) to raw timeseries (blue). Reconstructed timeseries generated from superposed cycles of 52, 11, and 8 days, and weighted in favour of the 52-day component based on a least-squares regression of the model to the raw timeseries ($A=3$, $B=1$, $C=1$; Section 2.1.2). (For interpretation of the references to colour in this figure legend, the reader is referred to the web version of this article.)

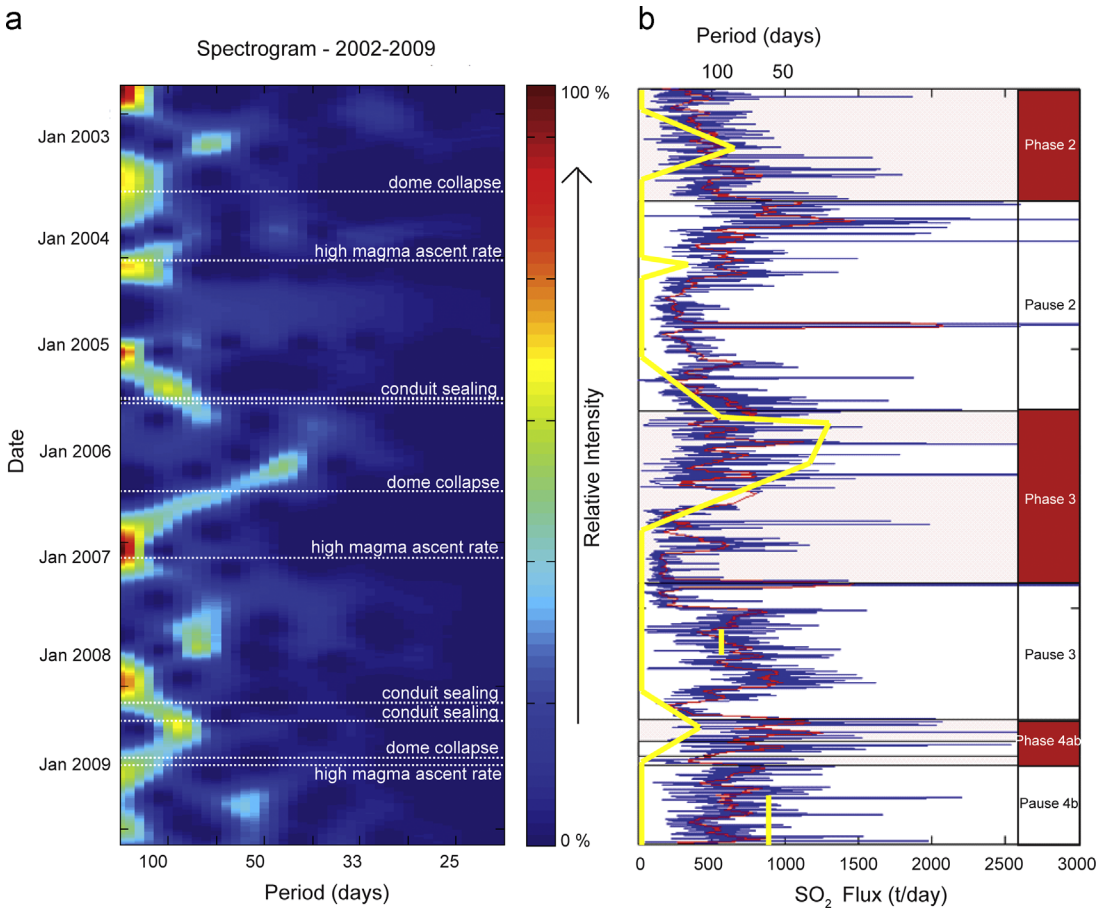


**Fig. 4.** (a) Spectrogram (2002–2009) compiled from power spectral density estimates over contiguous sub-sections of the total timeseries, plotted using a relative colourscale (warmer colours indicative of higher spectral power relative to other frequencies for a particular window). The figure illustrates temporal frequency variation for dominant cycles within the $SO_2$ flux timeseries with the occurrence of Vulcanian explosive events highlighted as white dotted lines for comparison (MVO chronology; see Section 4.1 for discussion). Each explosive event is labelled with the corresponding explosion mechanism, based on similar patterns in ground deformation, pyroclast textures and $SO_2$ flux (summarised in Table F, Supplementary information). It is possible that the use of a relative colourscale normalised to unity may obscure the trace of weaker cycles, which might be clearer if the scale is normalised to that of the dominant cycle. However our focus here is on the stronger cycles and so this plot is not explored. (b) $SO_2$ timeseries (2002–2009): $SO_2$ fluxes displayed as both the raw (blue) and 20-day smoothed (red) timeseries, with shaded regions corresponding to phases of active lava extrusion. The yellow curve illustrates the general features of the spectrogram trace over the same interval for qualitative comparison. (For interpretation of the references to colour in this figure legend, the reader is referred to the web version of this article.)

with significant dome collapse events. These results support earlier suggestions of cycle instability (Section 3.1) based on the broad character of several spectral peaks.

### 3.3. Short-term Fourier Transform (STFT) results

Reconstructive analysis of the SHV $SO_2$ flux (Section 3.2) has shown that cyclic components are often unstable, with intensities and/or periods that do not remain constant with time. Here, we use STFT analysis to explore this temporal variability and to investigate changes in cycle strength as a function of time.

The spectrogram (Fig. 4) clearly shows a modulation of the frequency distribution, illustrated by the oscillation of the band of strongest spectral power between ~0.02 cycles/day (period ~50 days) and a baseline saturated at very low frequencies (periods >100 days). The frequency peaks correspond to a period of approximately 50-days, and most likely reflect variation in the strength of the multi-week cycle, with peaks representing time intervals where this cyclicity is manifest most strongly in the $SO_2$ emissions. The intervals where the spectral power is saturated at very low frequencies may represent periods where the multi-week cycle is suppressed and/or the spectral density is swamped by long-period components acting over timescales greater than the window length.

Three main modulations of cycle frequency are distinguishable, along with two isolated regions of high spectral power (Fig. 4). The peak frequencies of these modulations vary from 0.017 to 0.025 cycles/day, reflecting a range in the absolute length of the multi-week cycle of 40–59 days. This variation is consistent with the results of the MTM analyses of individual phases, which suggest a range of 41–63 days (Table 1). The temporal agreement between spectrogram peaks and the intervals where a multi-week component provided the best model fit to the raw dataset (reconstructive modelling; Section 3.2 and Supplementary Fig. C) provides further evidence that the two methods are detecting the same cycle. The frequency maximum occurring late 2005 to early 2006 is significantly larger than other peaks, in both duration and frequency, and most clearly illustrates evolution in cyclic behaviour.

### 3.4. Multi-parameter cross-correlation results

The close similarity between periodic components evident in the $SO_2$ timeseries (41–63, 17–26, and 11–14 days; Table 1) and those documented previously at SHV in timeseries of seismicity, ground tilt, and lava efflux (6–8 weeks (or 42–56 days) and 11–16 days; e.g., Loughlin et al., 2010; Odbert et al., in press; Voight et al., 1998) suggests that these multiple parameters may be controlled by the same underlying process. To test this hypothesis, we

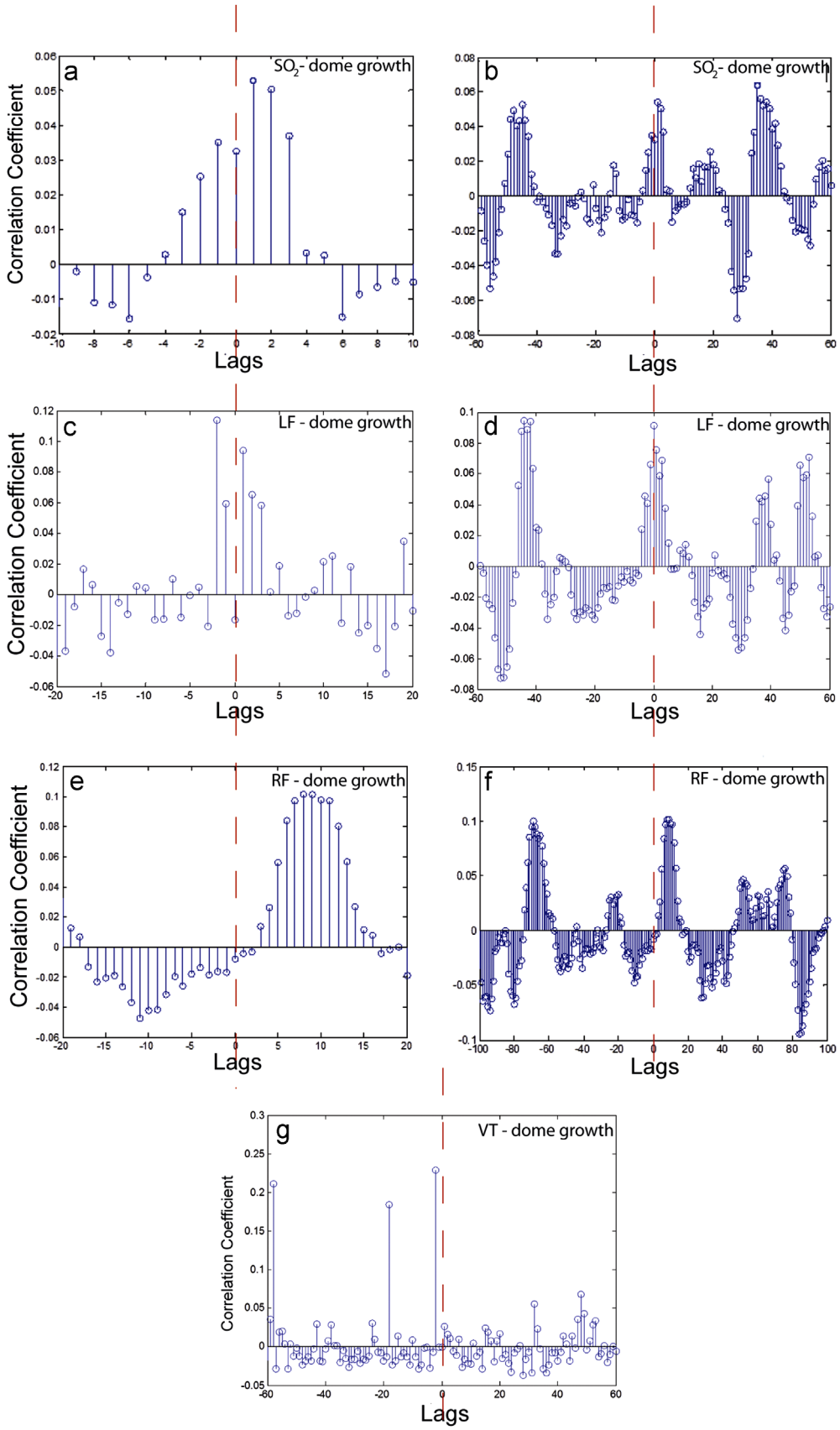


**Fig. 5.** Cross-correlation analysis between timeseries of $SO_2$ flux and both daily seismic event counts (including low-frequency (LF), volcano-tectonic (VT) and rockfall (RF) seismicity) and lava efflux for eruptive Phase 3 (Aug 2005-April 2007): continuous timeseries of $SO_2$/seismic counts held stationary, whilst binary timeseries of dome growth progressively offset by a multiples of the daily sampling frequency (lags). A hypothetical correlation maximum at lag=0 (dashed red line) indicates a simultaneous relationship between dome growth and degassing, while strong correlations at negative/positive lag values imply maxima in either degassing or seismicity precede/follow the onset of growth respectively; (a,b) $SO_2$-Dome Growth (5a highlights the short-term variation in correlation coefficient, whilst 5b extends the analysis to illustrate periodicity in correlation over a longer timescale); (c,d) LF-Dome Growth; (e,f) RF-Dome Growth; (g) VT-Dome Growth. (For interpretation of the references to color in this figure legend, the reader is referred to the web version of this article.)

investigated whether systematic temporal relationships exist between $SO_2$ flux, seismicity and lava efflux, on the timescales indicated by spectral analysis, using correlation analysis (Fig. 5; Supplementary information).

Seismic monitoring data at SHV is acquired at a high sampling rate from 10 broadband seismometers distributed around, and at various distances from, the volcano, and therefore represents an almost continuous timeseries (Luckett et al., 2007). Datasets of daily seismic event counts are generated from the raw seismic waveform, and record the cumulative number of each seismic event type (discriminated on the basis of the shape, frequency content and duration of the seismic waveform) occurring over a 24-h sampling interval. Datasets were prepared for cross-correlation analysis using a detrending correction to remove any correlations resulting from the finite length of the dataset, then truncated to a length equal to that specified for the $SO_2$ flux timeseries. In addition, Loughlin et al. (2010) documented several lava-dome 'growth cycles' based on changes in magma effusion rate during Phase 3. In the absence of a continuous daily time-series of effusion rates we use these growth cycles as a proxy for lava efflux, in the form of a binary timeseries (i.e. zeroes throughout, except on days corresponding the start of a growth cycle as defined by Loughlin et al., 2010).

Timeseries of $SO_2$ flux and daily seismic event counts have been compared for eruptive Phases 2 and 3 (July 2002–July 2003 and Aug 2005–April 2007 respectively), with dome growth data also incorporated for Phase 3. These intervals have been selected for analysis as they represent the periods where cyclic behaviour in both gas flux (Section 3.2) and seismicity, including low-frequency (LF), volcano-tectonic (VT) and rockfall (RF) events (Miller et al., 1998), is most clearly defined at timescales of ~50 days (Odbert et al., in press).

Fig. 6 summarises a synoptic framework of the lead–lag relationships between $SO_2$ flux, seismicity, and dome growth during Phases 2 and 3, based on the results of correlation analysis summarised in Table 3. Cyclicity in the strength of the correlation coefficient is evident on timescales of 30–50-days for each analysis, with the additional periodicities detected in the $SO_2$ flux timeseries (i.e. 10–14 days) not strongly manifest. This result is consistent with earlier results suggesting that this cycle is dominant (Section 3.1); therefore, we focus on the 50-day (multi-week) cycle in subsequent discussions. Elevated seismicity begins the sequence, typically in the form of an extended period of enhanced LF activity concurrent with a short-lived VT swarm. Initiation of new phases of dome extrusion (when applicable, i.e., for Phase 3 data) and $SO_2$ flux maxima occur after lags of ~2 and 4 days respectively following the seismic swarms, with gas fluxes having built gradually since the initial VT and LF swarms. Increasing RF activity climaxes ~7 days following the onset of extrusion, and then persists over several days. These patterns repeat over a period of 30–50 days. Although cross-correlation analysis has shown these relationships to be repeatable and generally self-consistent, Fig. 6 illustrates an idealised scenario representing average behaviour over the defined time interval.

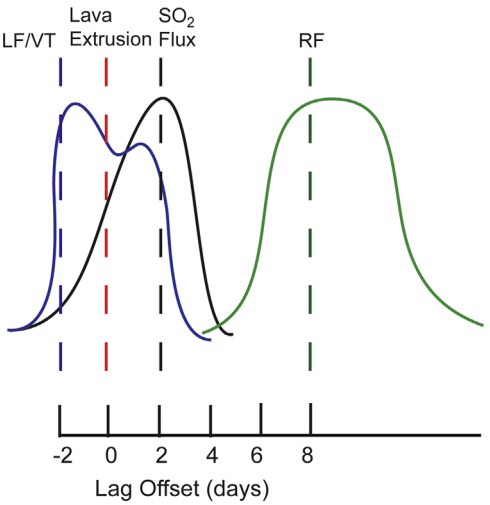


**Fig. 6.** Multi-parameter sequence relationships: lag offsets in timeseries of seismic event rate and gas flux along the *x*-axis are here expressed relative to the onset of magma extrusion. The relative magnitude of the correlation coefficient is displayed as a continuous variable, with peak correlation indicated by vertical dashed lines. A peak in low-frequency/volcano-tectonic seismic events (LF/VT; blue dashed line) defines the start of the sequence, followed by the onset of vigorous surface extrusion after days (red dashed line). Peak degassing lags the onset of lava extrusion by a further two days (black solid line), accompanied by a second, smaller, peak in LF event rate. Rockfall event rate climaxes approximately one week after the onset of lava extrusion (green dashed line), and remains elevated for several days. (For interpretation of the references to colour in this figure legend, the reader is referred to the web version of this article.)

## 4. Discussion

### 4.1. Temporal evolution in multi-week cyclicity

Our results reveal complex degassing patterns at Soufrière Hills Volcano, with MTM analyses (Section 3.1) providing evidence for cyclicity on multiple superposed timescales during 2002–2011. Furthermore, both reconstructive analysis (Section 3.2) and STFT analysis (Section 3.3) indicate that the expression of cyclic behaviour in the surface gas flux varies distinctly when studied as a function of time.

Temporal fluctuation in cyclic behaviour may be attributed to a fundamental change in either gas source processes, or in the subsequent transport of $SO_2$ to the surface (Odbert and Wadge, 2009). In Section 3.3, we suggest that the dominant frequency modulation identified within the $SO_2$ timeseries spectrogram reflects variation in the amplitude (or strength) of the multi-week cycle. It is cyclicity on this timescale that is consistently most clearly manifest throughout all analyses, including the timeseries reconstructions presented in Section 3.2 (which must be weighted in favour of the ~50-day component to optimise the fit to the data), and so is the focus of all further discussion; the resolution of the $SO_2$ dataset is insufficient to allow detailed interpretations of cyclic components at higher frequencies. The spectrogram shown in Fig. 4 has been directly compared to timeseries of other parameters (e.g., multi-year variation in $SO_2$ flux magnitude, phases of active dome growth) to explore potential systematic relationships between the strength of multi-week cyclicity and eruptive behaviour. This comparison offers valuable insights into the conditions under which cyclic behaviour is most favourable, thereby helping to constrain the origin of the cycles.

#### 4.1.1. Influence of magma ascent and total gas flux

If active magma ascent was the sole control on cycle amplitude, then we may expect sustained periodic behaviour throughout active extrusion, and weakening during eruptive pauses. However, comparing the shape of the frequency modulation to magmatic extrusion cycles (shaded regions of Fig. 4) reveals no simple systematic relationship. Although most periods where the multi-week cycle is strong occur during phases of active extrusion, this is not the rule; episodes of multi-week cyclicity are generally not sustained, and are also observed without dome growth. This supports the observation that $SO_2$ transport is decoupled from magma extrusion over long timescales (Christopher et al., 2010; Edmonds et al., 2003a, 2010).

**Table 3**
Summary of correlation results: the number of 'lags' refers to the offset (in multiples of the daily sampling frequency) required to align peaks in one timeseries (listed vertically) with those of the other (listed horizontally). Note that positive/negative lags imply the vertically listed parameter precedes/follows the horizontal parameter respectively.

| Cross-correlation parameters | $SO_2$ | | | | Dome growth | |
|---|---|---|---|---|---|---|
| | Phase 2 | | Phase 3 | | Phase 3 | |
| | Maximum correlation[a] (lags) | Correlation cyclicity[b] (lags) | Maximum correlation[a] (lags) | Correlation cyclicity[b] (lags) | Maximum correlation[a] (lags) | Correlation cyclicity[b] (lags) |
| **$SO_2$** | – | – | – | – | 1–2 | 40–50 |
| **LF** | (−1) –9 | 40–50 | (−4) –8 | 40–60 | (−2)–3 | 40–50 |
| **VT** | 0 | ~20 | –9 and 8 | ~20 | −2 | – |
| **RF** | (−16) and 13 | 30–40 | 1–12 | 50–60 | 7–11 | 30–40 |

[a] 'Maximum correlation' refers to the lag offset required to align peaks in the two timeseries.
[b] 'Correlation cyclicity' refers to the time interval between successively aligned peaks.

Equally, inferring any relationship between multi-week cycle strength and the long-term 2–3 yr $SO_2$ flux cycles, based on overlaying the spectrogram trace onto the $SO_2$ flux timeseries (Fig. 4b), is ambiguous. This null result supports the idea that the multi-year cycles in surface gas flux originate from deeper in the system (Christopher et al., 2010), and are thus relatively independent of conduit processes that may generate the multi-week cyclicity (processes involved discussed in Section 4.2).

#### 4.1.2. Influence of explosive activity

Abrupt transitions between effusive, explosive and paused activity are characteristic of intermediate dome-forming eruptions (Melnik and Sparks, 2005) and reflect rapidly changing conditions within the conduit, which would also influence or be influenced by the nature of gas ascent. On Montserrat, seismic event rates have been observed to accelerate prior to explosive behaviour, with a subsequent deceleration following the cessation of activity (Kilburn and Voight, 1998; Neuberg et al., 2006). Here we test the hypothesis that the amplitude and/or frequency of the multi-week cyclical component in the gas flux exhibit a similarly systematic response.

Explosive events at SHV (2002–2009) are highlighted in Fig. 4, and a comparison to the PSD distribution indicates a slight clustering of explosive behaviour during either a period of escalation in cycle frequency (i.e., a strengthening of the multi-week cycle; 29 May 2005, 29 July 2008) or directly prior to a decline (e.g., 20 May 2006, 2 Dec 2008). Since the window overlap used to calculate Fig. 4 precludes more exact temporal correlation, several events have been considered in more detail using finer resolution spectrograms (Fig. 7; refer to the sensitivity study presented in Supplementary information for discussion of parameter selection, such as window length).

Consideration of both the dynamics of each explosion, revealed by strain modelling and examination of eruptive products, as well as the eruptive context in terms of magmatic extrusion, may help to elucidate the relationship between conduit conditions and cyclic behaviour. Vulcanian explosions at SHV have typically occurred in episodic cycles, or in isolation either during eruptive pauses or directly following dome collapses (Edmonds and Herd, 2007; Komorowski et al., 2010; Voight et al., 1999). Explosive activity is a reflection of conditions within the conduit, specifically the balance between degassing rates and pressurisation (Diller et al., 2006; Herd et al., 2005; Melnik and Sparks, 2005). The specific conditions pertaining to each event must therefore be considered independently before drawing conclusions regarding a relationship between cyclic degassing and explosive behaviour (Table F, Supplementary information; labelled in Fig. 4a).

Several systematic observations from STFT analysis (Figs. 4 and 7) support the hypothesis that changes in the nature of cyclic degassing are directly linked to explosive behaviour:

(1) Events attributed to large-scale dome collapse and depressurisation (Herd et al., 2005; supported by strainmeter observations e.g., Voight et al., 2006), are often preceded by a period of cycle stability, during which the multi-week cycle is most apparent in the gas signal. An abrupt deceleration in cycle frequency, and a breakdown of the multi-week cyclic component, coincides with collapse. This is most clearly illustrated by the dome collapse events of 20 May 2006 and 12 July 2003 (Figs. 4a and 7a, c; note that these two events represent the only two examples of complete collapse of the dome edifice to date).
(2) Several isolated explosive events (e.g., January 2007 and March 2004, labelled high magma ascent rate; Figs. 4a and 7b, d) appear to occur in the absence of any strong cyclicity; both examples occur in the months following the breakdown in cyclicity associated with dome collapse events. It is likely that the January 2007 event was the result of pyroclastic flows eroding into the northern face of the dome, over a period leading up to the explosion (Christopher, T., *unpublished data*).
(3) Conduit sealing, or more specifically the failure of the seal, has been invoked based largely on the analysis of eruptive products (Komorowski et al., 2010) to explain several Vulcanian explosions occurring following significant intervals of reduced gas flux (e.g., May–July 2008 and 29 May 2005; Fig.4). In contrast to the breakdown in cyclic degassing triggered by collapse, explosive behaviour of this style appears to correlate with increases in apparent cycle frequency following periods of suppressed cyclicity, and hence a strengthening of the multi-week periodicity.

These observations suggest that the occurrence of explosive activity may modulate either the source process of the multi-week cycle itself, or the strength of the manifestation of this process in the $SO_2$ flux.

### 4.2. Physical mechanisms controlling cyclicity

Periodicities evident in the $SO_2$ flux match those identified at SHV in other geophysical timeseries. We propose, based on the lead–lag relationships between seismicity, dome growth and degassing presented in Section 3.4, that cyclicity in each of these parameters may be subject to a common source process. The onset of magma extrusion (Phase 3), peak degassing and elevated rockfall were shown to lag initial low-frequency/volcano-tectonic (LF/VT) swarm seismicity by ~2, 4, and 7 days respectively: a

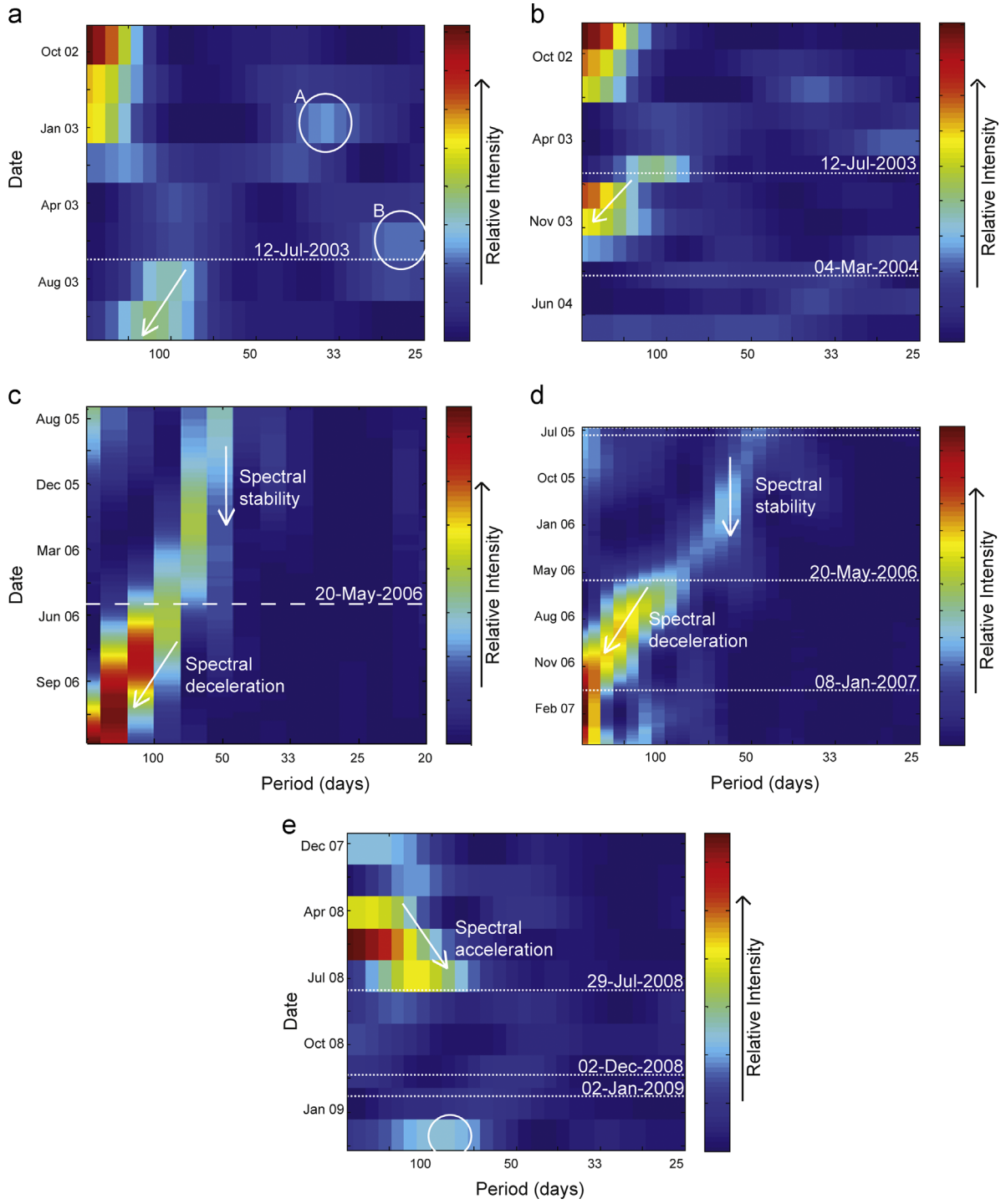


**Fig. 7.** Short-term Spectrograms: (a) Phase 2 (September 2002–September 2003); (b) Phase 2 expanded (September 2003–July 2004); (c) Phase 3 (August 2005–October 2006); (d) Phase 3 expanded (July 2005–March 2007); (e) Phase 4 (December 2007–February 2009). Relative intensity from 0% (blue) to 100% (red).Long-period cycles dominate the frequency distribution so that cycle periods less than ~25 days are not distinguishable using the relative colourscale. Significant trends in the strength of the multi-week cyclicity are annotated, whilst circles highlight regions of isolated high spectral power. (For interpretation of the references to colour in this figure legend, the reader is referred to the web version of this article.)

sequence recurrent on timescales of 30–50 days during Phases 2 and 3.

The observed lag of 0–2 days between the initiation of LF swarms and exogenous growth during Phase 3 may reflect the ascent time required for the magma pulse to reach the surface from seismic source depths. A simple calculation, based on our observed two-day lead time and a source depth of 1.0–1.5 km (assuming the LF swarm is generated by fluid motion associated with magma microfracturing during ascent at the dyke-conduit transition; Thomas and Neuberg, 2012), yields approximate magma ascent rates of $6–9 \times 10^{-3}$ ms$^{-1}$ in the shallow conduit. This is consistent with reported ascent rates at both SHV and Mt St Helens of $10^{-4}$–$10^{-2}$ ms$^{-1}$ based on petrological methods (Devine et al., 1998; Rutherford and Hill, 1993). The sustained LF activity (Fig. 5c) is consistent with the continued acceleration of magma over several days.

The development of instabilities in the dome edifice is intimately linked to magma extrusion dynamics, with the onset of rapid localised dome growth resulting in oversteepened, metastable regions prone to failure (Calder et al., 2002). Small individual collapse events manifest as elevated RF activity, and so the observed lag of ~7 days between initial extrusion and the peak in RF events (Fig. 5) may reflect the time required to destabilise the edifice.

The broadly simultaneous correlation between dome growth and the occurrence of LF seismic swarms is consistent with a scenario in which enhanced marginal shear strains associated with periodic high magma ascent rates lead to corresponding cyclic pulses of increased low-frequency seismicity (Costa et al., 2007a,b; Thomas and Neuberg 2012). However, the mechanisms linking degassing cycles to those of lava efflux and seismicity are less clear. Collinson and Neuberg (2012) suggest gas flux is controlled by a complex interplay between the structure, permeability and pressure distribution within the conduit.

The correlation analysis presented in Section 3.4 demonstrates that, while sequential offsets between each parameter are observed over periods of ~10 days (which reveal subtle evolutionary patterns in eruptive behaviour), degassing peaks are broadly concurrent with both enhanced swarm seismicity and more vigorous magma efflux when correlations are considered over longer timescales (Fig. 5); maximum gas ascent rates thus appear in step with, but systematically offset from, magma efflux. Experimental work has demonstrated that bubble shear-coalescence, and hence the development of magmatic permeability, is enhanced during the conditions of maximum shear associated with elevated magma ascent rates (e.g., Okumura et al., 2006, 2008). The apparent co-variance between $SO_2$ emissions and magma extrusion may therefore suggest that the development of permeability, rather than overpressure, represents the dominant control on gas ascent over multi-week timescales of ~50-days. This is supported by modelling of the multi-week periodicity at SHV that predicts conditions of minimum overpressure concurrent with maximum extrusion rates (Costa et al., 2007a,b, 2013).

Invoking shear-coalescence during enhanced magma ascent as the dominant control on surface gas flux cannot reconcile all observations, however. Relationships between $SO_2$ flux and seismicity exist, and exhibit the 40–50 day repeat time, even when analysis is restricted to early Phase 3 when no clear growth cycles are documented (Loughlin et al., 2010). While it is possible that an endogenous growth mode could explain the cyclicity during the early dome-building stages of Phase 3 (Loughlin et al., 2010), this does not account for either the qualitative decoupling of gas flux from the 2 to 3 yr phases of magmatic extrusion (Fig. 1; Edmonds et al., 2010) or the evidence for multi-week cyclicity in $SO_2$ emissions during both active and paused dome growth (Sections 3.1 and 4.1). These observations imply that although a bubble shear-permeability control on gas ascent is an attractive solution during phases of dome growth, other mechanisms (i.e. development of fracture networks; Jaupart, 1998; Sparks et al., 2000) must be invoked to explain degassing in the absence of magmatic extrusion.

Furthermore, any mechanism proposed to explain degassing cycles must be able to account for the observed temporal variation in cyclicity (Section 3.3). An absence of periodic behaviour in surface gas flux does not necessarily preclude pulsatory gas ascent deeper in the conduit. For example, during extended intervals of low $SO_2$ emissions (i.e., conduit 'sealing'; Edmonds et al., 2003a; Komorowski et al., 2010), the shallow conduit is effectively impermeable to vertical gas transport and hence results in gas storage beneath the seal. Variations in the $SO_2$ flux originating below this depth would thus be damped, suppressing the cyclic signature in surface gas measurements. This may explain the absence of any significant periodic signal in the gas flux data over the months prior to the December 2002, 29 May 2005 and May–July 2008 explosions (Fig. 4). Strain modelling (Chardot et al., 2010) and estimates of total erupted volume (Komorowski et al., 2010) both indicate conduit excavation to depths of ~1 km during these events, sufficient to remove the impermeable plug. This would allow cycles of permeability development to be freely expressed in the surface gas flux, highlighted most clearly by the rapid strengthening of the multi-week component following the 29 May 2005 explosion.

Nevertheless, any further interpretations remain highly speculative. We conclude that the controls on gas ascent are complex, and cannot be attributed to a single variable.

Although recent numerical models have begun to investigate the complex permutations of permeability and pressure required to promote either gas storage or escape (Collinson and Neuberg, 2012), a consideration of the mechanisms leading to cyclic behaviour, perhaps extending the approach of Costa et al. (2007a,b) to account for more general gas transport mechanisms, is needed in order to explore the apparent systematic relationship between the strength of cyclical degassing and both the occurrence and style of explosive activity at SHV.

## 5. Conclusions

Timeseries analysis of the long-term daily-averaged $SO_2$ flux from Soufrière Hills Volcano, Montserrat, has provided insights into the nature of cyclic behaviour at a resolution comparable to that possible for seismic and deformation datasets from volcanoes for the first time. $SO_2$ emissions at SHV exhibit complex cyclic behaviour on a variety of timescales, many of which persist throughout phases of both active extrusion and eruptive pause, and show close similarities to periodic components identified in other geophysical parameters. Cyclicity over 2–3 yr, 6–8 weeks (~50 days), and 10–14 days was evident in analyses of the complete timeseries (2002–2009), as well as in those of individual phases. The multi-week cycle on timescales of ~50 days exceeded the highest confidence level of the red noise model throughout most of the eruption, suggesting that it represents a fundamental property of the degassing regime.

The results of spectral timeseries analysis, using Multitaper Fast-Fourier Transform (FFT), were cross-checked using reconstructive analysis, which supported the hypothesis that the $SO_2$ timeseries could be approximated by superposition of multiple periodicities, weighted in favour of the multi-week cycle. Timeseries reconstructions also reaffirmed that cycle periods do not always remain stable at SHV, and highlighted the need to relate spectral results back to the raw timeseries in order to fully characterise the cyclicity.

The relationships between $SO_2$ flux, seismic event counts, and dome-growth during Phases 2 and 3 have been explored and quantified by correlation analysis. Results support rejection of the null hypothesis that each timeseries varies independently, in favour of a scenario involving multi-parameter feedbacks. Peaks in $SO_2$ flux appear to correspond broadly to enhanced lava extrusion and elevated seismicity within cycles of 30–50 days. However, time lags of 2, 4 and 7 days are observed between initial low-frequency seismic swarms and peaks in dome growth, $SO_2$ flux and rockfall event rate respectively. Although this analysis offers valuable insights into the controls on subsurface gas ascent, deconvolving the relative contributions of permeability and overpressure, as well as other factors, remains challenging and requires further research.

Short-term Fourier Transform (STFT) analysis utilised the observed temporal variation to explore changes in the strength

of each cyclic component with time. The multi-week periodicity (with cycle periods of ~50-days) exhibits distinct temporal variation, including abrupt changes in both strength and period, which appears largely systematic with respect to eruptive activity. Comparison between the strength of the multi-week periodicity and the occurrence of specific styles of explosive activity suggests that the manifestation of cyclicity in surface gas flux is itself modulated by the influence of large-scale eruptive phenomena on the physical conditions within the conduit.

These observations at SHV of cyclicity in gas flux, temporal correlations with other geophysical datastreams and systematic variations in the nature of the cyclicity with volcanic behaviour offer new constraints on subsurface processes. Understanding the full implications will require new efforts including the development of models of conduit mechanisms to incorporate quantitative measures of degassing and to explore the feedbacks that influence the temporal expression of cyclicity in surface gas flux.

Comparative studies at other volcanoes are of great importance. Cyclic deformation and seismicity observed at other dome-forming systems is often comparable to that of SHV, suggesting similar source mechanisms. Therefore, other degassing regimes may also exhibit similar periodic behaviour (e.g., Holland et al., 2011). Although based upon measurements from SHV, this study suggests that applying timeseries analysis to high-temporal-resolution gas flux measurements and other geophysical datastreams at other volcanoes may provide an effective method both to characterise patterns of degassing and to learn more about the underlying controls on volcanic behaviour.

## Acknowledgements

We thank the staff of the Montserrat Volcano Observatory for assistance in data collection and processing, and for access to geophysical datasets. EJN acknowledges financial support from The Mineralogical Society, Lydia Press Foundation, Richard Hale Association and University College Oxford. This work was completed with support for DMP and TAM from the NERC-ESRC grant STREVA (NE/J020001/1 and NE/J020052/1) and the NCEO, of which the Centre for the Observation and Modelling of Earthquakes, Volcanoes and Tectonics (COMET+) is a part. We also thank two anonymous reviewers for their valuable comments that greatly improved this manuscript.

## Appendix A. Supplementary material

Supplementary data associated with this article can be found in the online version at http://dx.doi.org/10.1016/j.epsl.2013.05.032.

## References

Aiuppa, A., Cannata, A., Cannavo, F., Di Grazia, G., Ferrari, F., Giudice, G., Gurrieri, S., Liuzzo, M., Mattia, M., Montalto, P., Patanè, D., Puglisi, G., 2010. Patterns in the recent 2007-2008 activity of Mount Etna volcano investigated by integrated geophysical and geochemical investigations. Geochem. Geophys. Geosyst. 11, Q09008.

Anderson, K., Lisowski, M., Segall, P., 2010. Cyclic ground tilt associated with the 2004–2008 eruption of Mount St. Helens. J. Geophys. Res. 115, B11201.

Barmin, A., Melnik, O., Sparks, R., 2002. Periodic behaviour in lava dome eruptions. Earth Planet. Sci. Lett. 199, 173–184.

Bonaccorso, A., Caltabiano, T., Currenti, G., Del Negro, C., Gambino, S., Ganci, G., Giammanco, S., Greco, F., Pistorio, A., Salerno, G., Spampinato, S., Boschi, E., 2011. Dynamics of a lava fountain revealed by geophysical, geochemical and thermal satellite measurements: the case of the 10 April 2011 Mt Etna eruption. Geophys. Res. Lett. 38, L24307.

Calder, E.S., Luckett, R., Sparks, R.S.J., Voight, B., 2002. Mechanisms of lava dome instability and generation of rockfalls and pyroclastic flows at Soufrière Hills Volcano, Montserrat. In: Druitt, T.H., Kokelaar, P.B. (Eds.), The Eruption of Soufrière Hills Volcano, Montserrat, from 1995 to 1999, vol. 21. Memoirs Geological Society, London, pp. 173–190.

Chardot, L., Voight, B., Foroozan, R., Sacks, S., Linde, A., Stewart, R., Hidayat, D., Clarke, A., Elsworth, D., Fournier, N., Komorowski, J.C., Mattioli, G., Sparks, R.S.J., Widiwijayanti, C., 2010. Explosion dynamics from strainmeter and microbarometer observations, Soufrière Hills Volcano, Montserrat: 2008–2009. Geophys. Res. Lett. 37, L00E24.

Christopher, T., Edmonds, M., Humphreys, M.C.S., Herd, R.A., 2010. Volcanic gas emissions from Soufrière Hills Volcano, Montserrat 1995–2009, with implications for mafic magma supply and degassing. Geophys. Res. Lett. 37, L00E04.

Collinson, A.S.D., Neuberg, J.W., 2012. Gas storage, transport and pressure changes in an evolving permeable volcanic edifice. J. Volcanol. Geotherm. Res. 243–244, 1–13.

Connor, C.B., Sparks, R.S.J., Mason, R.M., Bonadonna, C., Young, S.R., 2003. Exploring links between physical and probabilistic models of volcanic eruptions: the Soufrière Hills Volcano, Montserrat. Geophys. Res. Lett. 30, 1701.

Costa, A., Melnik, O., Sparks, R.S.J., 2007a. Controls of conduit geometry and wallrock elasticity on lava dome eruptions. Earth Planet. Sci. Lett. 260, 137–151.

Costa, A., Melnik, O., Sparks, R.S.J., Voight, B., 2007b. Control of magma flow in dykes on cyclic lava dome extrusion. Geophys. Res. Lett. 34, L02303.

Costa, A., Wadge, G., Melnik, O., 2012. Cyclic extrusion of a lava dome based on a stick-slip mechanism. Earth Planet. Sci. Lett. 337–338, 39–46.

Costa, A., Wadge, G., Stewart, R., Odbert, H., 2013. Coupled sub-daily and multi-week cycles during the lava dome eruption of Soufrière Hills Volcano, Montserrat. J. Geophys. Res 2169-9356.

Denlinger, R., Hoblitt, R., 1999. Cyclic eruptive behaviour of silicic volcanoes. Geology 27, 459–462.

Devine, J. D., Murphy, M. D., Rutherford, M. J., Barclay, J., Sparks, R. S. J., Carroll, M. R., Young, S. R., Gardner, J. E., 1998. Petrologic evidence for pre-eruptive pressure-temperature conditions, and recent reheating, of andesitic magma erupting at the Soufriere Hills Volcano, Montserrat, W.I. Geophys. Res. Lett. 25, 1944-80.

Diller, K., Clarke, A.B., Voight, B., Neri, A., 2006. Mechanisms of conduit plug formation: implications for Vulcanian explosions. Geophys. Res. Lett. 33, L20302.

Druitt, T.H., Kokelaar, P.B., 2002. The Eruption of Soufrière Hills Volcano, Montserrat, from 1995 to 1999. vol. 21. Geological Society, London, Memoirs.

Edmonds, M., Pyle, D.M., Oppenheimer, C., 2001. A model for degassing at the Soufrière Hills Volcano, Montserrat, West Indies, based on geochemical data. Earth Planet. Sci. Lett. 186, 159–173.

Edmonds, M., Oppenheimer, C., Pyle, D.M, Herd, R., Thompson, G., 2003a. $SO_2$ emissions from Soufrière Hills Volcano and their relationship to conduit permeability, hydrothermal interaction and degassing regime. J. Volcanol. Geotherm. Res. 124, 23–43.

Edmonds, M., Herd, R.A., Galle, B., Oppenheimer, C.M., 2003b. Automated, high time-resolution measurements of $SO_2$ flux at Soufrière Hills Volcano, Montserrat. Bull. Volcanol. 65 (8), 578–596.

Edmonds, M., Herd, R.A., 2007. A volcanic degassing event at the explosive–effusive transition. Geophys. Res. Lett. 34, L21310.

Edmonds, M., Aiuppa, A., Humphreys, M., Moretti, R., Giudice, G., Martin, R.S., Herd, R.A., Christopher, T., 2010. Excess volatiles supplied by mingling of mafic magma at an andesite arc volcano. Geochem. Geophys. Geosyst. 11, Q04005.

Foroozan, R., Elsworth, D., Voight, B., Mattioli, G., 2011. Magmatic-metering controls the stopping and restarting of eruptions. Geophys. Res. Lett. 38, L05306.

Ghil, M., Allen, M., Dettinger, M., Ide, K., Kondrashov, D., Mann, M., Robertson, A., Saunders, A., Tian, Y., Varadi, F., Yiou, P., 2002. Advanced spectral methods for climatic time series. Rev. Geophys. 40, 1003.

Harris, A.J., Rose, W.I., Flynn, L.P., 2003. Temporal trends in lava dome extrusion at Santiaguito (1922–2000). Bull. Volcanol. 65, 77–89.

Herd, R., Edmonds, M., Bass, V., 2005. Catastrophic lava dome failure at Soufrière Hills Volcano, Montserrat, 12–13 July 2003. J. Volcanol. Geotherm. Res. 148, 234–252.

Holland, A.S.P., Watson, I.M., Phillips, J.C., Caricchi, L., Dalton, M.P., 2011. Degassing processes during lava dome growth: insights from Santiaguito lava dome, Guatemala. J. Volcanol. Geotherm. Res. 202, 153–166.

Jaupart, C., 1998. Gas loss from magmas though conduit walls during eruption. In: Gilbert, J.S., Sparks, R.S.J. (Eds.), The Physics of Explosive Volcanic Eruptions, vol. 145. Geological Society, London, Special Publication, pp. 73–90.

Jaquet, O., Sparks, R.S.J., Carniel, R., 2006. Magma memory recorded by statistics of volcanic explosions at the Soufrière Hills Volcano, Montserrat. In: Mader, H.M., Coles, L.J., Connor, C.B., Connor, L.J. (Eds.), Statistics in Volcanology. IAVCEI, pp. 175–184.

Kilburn, C., Voight, B., 1998. Slow rock fracture as eruption precursor at Soufrière Hills Volcano, Montserrat. Geophys. Res. Lett. 25, 3665–3668.

Komorowski, J.C., Legendre, Y., Christopher, T., Bernstein, M., Stewart, R., Joseph, E., Fournier, N., Chardot, L., Finizola, A., Wadge, G., Syers, R., Williams, C., Bass, V., 2010. Insights into processes and deposits of hazardous vulcanian explosions at Soufrière Hills Volcano during 2008 and 2009 (Montserrat, West Indies). Geophys. Res. Lett. 37, L00E19.

Landi, P., Marchetti, E., La Felice, S., Ripepe, M., Rosi, M., 2011. Integrated petrochemical and geophysical data reveals thermal distribution of the feeding conduits at Stromboli volcano, Italy. Geophys. Res. Lett. 38, L08305.

Lensky, N.G., Sparks, R.S.J., Navon, O., Lyakhovsky, V., 2008. Cyclic activity at Soufrière Hills Volcano, Montserrat: degassing-induced pressurization and stick-slip extrusion. 307. Geological Society, London, Special Publication, pp. 169–188.

Loughlin, S.C., Luckett, R., Ryan, G., Christopher, T., Hards, V., De Angelis, S., Jones, L., Strutt, M., 2010. An overview of lava dome evolution, dome collapse and cyclicity at Soufrière Hills Volcano, Montserrat, 2005–2007. Geophys. Res. Lett. 37, L00E16.

Luckett, R., Baptie, B., Ottemoller, L., Thompson, G., 2007. Seismic monitoring of the Soufrière Hills Volcano, Montserrat. Seismol. Res. Lett. 78, 192–200.

Mann, M., Lees, J., 1996. Robust estimation of background noise and signal detection in climatic timeseries. Climatic Change 33, 409–445.

Matthews, S., Gardeweg, M., Sparks, R., 1997. The 1984 to 1996 cyclic activity of Lascar volcano, northern Chile: cycles of dome growth, dome subsidence, degassing and explosive eruptions. Bull. Volcanol. 59, 72–82.

Matthews, A.J., Barclay, J., Johnstone, J.E., 2009. The fast response of volcano-seismic activity to intense precipitation: triggering of primary volcanic activity by rainfall at Soufrière Hills Volcano, Montserrat. J. Volcanol. Geotherm. Res. 184, 405–415.

Melnik, O., Sparks, R., 1999. Nonlinear dynamics of lava dome extrusion. Nature 402, 37–41.

Melnik, O., Sparks, R., 2005. Controls on conduit magma flow dynamics during lava dome building eruptions. J. Geophys. Res. 110, B02209.

Miller, A., Stewart, R., White, R., Luckett, R., Baptie, B., Aspinall, W., Latchman, J., Lynch, L., Voight, B., 1998. Seismicity associated with dome growth and collapse at the Soufrière Hills Volcano, Montserrat. Geophys. Res. Lett. 25, 3401–3404.

Neuberg, J., Tuffen, H., Collier, L., Green, D., Powell, T., Dingwell, D., 2006. The trigger mechanism of low-frequency earthquakes on Montserrat. J. Volcanol. Geotherm. Res. 153, 37–50.

Newhall, C.G., Melson, W.G., 1983. Explosive activity associated with the growth of volcanic domes. J. Volcanol. Geotherm. Res. 17, 111–131.

Odbert, H.M., Wadge, G., 2009. Timeseries analysis of lava flux. J. Volcanol. Geotherm. Res. 188, 305–314.

Odbert, H.M., Stewart, R.C, Wadge, G. Cyclic Phenomena at the Soufrière Hills Volcano, Montserrat (in press).

Okumura, S., Nakamura, M., Tsuchiyama, A., 2006. Shear-induced bubble coalescence in rhyolitic melts with low vesicularity. Geophys. Res. Lett. 33, L20316.

Okumura, S., Nakamura, M., Tsuchiyama, A., Nakano, T., Uesugi, K., 2008. Evolution of bubble microstructure in sheared rhyolite: formation of a channel-like bubble network. J. Geophys. Res. 113, B06201.

Pearson, S.C.P., Connor, C.B., Sanford, W.E., 2008. Rapid response of a hydrologic system to volcanic activity: Masaya volcano, Nicaragua. Geology 36, 951–954.

Percival, D., Walden, A., 1993. Spectral Analysis for Physical Applications: Multitaper and Conventional Univariate Techniques. Cambridge University Press.

Pyle, D.M., 1998. Forecasting sizes and repose times of future extreme volcanic events. Geology 26, 367–370.

Rutherford, M., Hill, P., 1993. Magma Ascent Rates from amphibole breakdown—an experimental study applied to the 1980–1986 Mount St Helens eruptions. J. Geophys. Res. 98, 19667–19685.

Sahetapy-Engel, S.T.M., Flynn, L.P., Harris, A.J.L., Bluth, G.J., Rose, W.I., Matias, O., 2004. Surface temperature and spectral measurements at Santiaguito lava dome, Guatemala. Geophys. Res. Lett. 31, 1944–8007.

Sparks, R.S.J., 1997. Causes and consequences of pressurisation in lava dome eruptions. Earth Planet. Sci. Lett. 150, 177–189.

Sparks, R.S.J., Murphy, M.D, LeJeune, A.M., Watts, R.B., Barclay, J., Young, S.R., 2000. Control on the emplacement of the andesite dome of the Soufrière Hills Volcano, Montserrat, by degassing-induced crystallisation. Terra Nova 12, 14–20.

Sparks, R.S.J., Aspinall, W.P., 2004. Volcanic activity: frontiers and challenges in forecasting, prediction, and risk assessment. In: Sparks, R.S.J., Hawkesworth, C.J. (Eds.), The State of the Planet: Frontiers and Challenges in Geophysics, 150. AGU Geophysical Monograph, pp. 359–371.

Swanson, D., Holcomb, R., 1990. Regularities in growth of the Mount St Helens dacite dome, 1980–1986. In: Fink, J.H. (Ed.). Lava Flows and Domes: Emplacement Mechanisms and Hazard Implications. IAVCEI Proceedings in Volcanology, 2, pp. 3–24.

Thomas, M., Neuberg, J., 2012. What makes a volcano tick. A first explanation of deep multiple seismic sources in ascending magma. Geology 40, 351–354.

Thomson, D.J., 1982. Spectrum estimation and harmonic analysis. Proc. IEEE 70, 1055–1096.

Voight, B., Hoblitt, R., Clarke, A., Lockhart, A., Miller, A., Lynch, L., McMahon, J., 1998. Remarkable cyclic ground deformation monitored in real-time on Montserrat, and its use in eruption forecasting. Geophys. Res. Lett. 25, 3405–3408.

Voight, B., Sparks, R., Miller, A., Stewart, R., Hoblitt, R., Clarke, A., Ewart, J., Aspinall, W., Baptie, B., Calder, E., Cole, P., Druitt, T., Hartford, C., Herd, R., Jackson, P., Lejeune, A., Lockhart, A., Loughlin, S., Luckett, R., Lynch, L., Norton, G., Robertson, R., Watson, I., Watts, R., Young, S., 1999. Magma flow instability and cyclic activity at Soufrière Hills Volcano, Montserrat, British West Indies. Science 283, 1138–1142.

Voight, B., Linde, A., Sacks, I., Mattioli, G., Sparks, R., Elsworth, D., Hidayat, D., Malin, P., Shalev, E., Widiwijayanti, C., Young, S., Bass, V., Clarke, A., Dunkley, P., Johnston, W., McWhorter, N., Neuberg, J., Williams, P., 2006. Unprecedented pressure increase in deep magma reservoir triggered by lava-dome collapse. Geophys. Res. Lett. 33, L03312.

Wadge, G., Herd, R., Ryan, G., Calder, E.S., Komorowski, J.C., 2010. Lava production at Soufrière Hills Volcano, Montserrat: 1995–2009. Geophys. Res. Lett. 37, L00E03.

Watson, I., Oppenheimer, C., Voight, B., Francis, P., Clarke, A., Stix, J., Miller, A., Pyle, D., Burton, M., Young, S., Norton, G., Loughlin, S., Darroux, B., 2000. The relationship between degassing and ground deformation at Soufrière Hills Volcano, Montserrat. J. Volcanol. Geotherm. Res. 98, 117–126.

Watt, S.F.L., Mather, T.A., Pyle, D.M., 2007. Vulcanian explosion cycles: patterns and predictability. Geology 35, 839–842.

Watts, R.B., Herd, R.A., Sparks, R.S.J., Young, S.R., 2002. Growth patterns and emplacement of the andesitic lava dome at Soufrière Hills Volcano, Montserrat. In: Druitt, T.H., Kokelaar, P. (Eds.), The Eruption of Soufrière Hills Volcano, Montserrat from 1995 to 1999 (2002), vol. 21. Geol. Soc., London, Mem., pp. 115–152.

Young, S., Sparks, R., Aspinall, W., Lynch, L., Miller, A., Robertson, R., Shepherd, J., 1998. Overview of the eruption of Soufrière Hills Volcano, Montserrat, 18 July 1995 to December 1997. Geophys. Res. Lett. 25, 3389–3392.

Young, S.R., Voight, B., Duffell, H.J., 2003. Magma extrusion dynamics revealed by high-frequency gas monitoring at Soufriere Hills Volcano, Montserrat. In: Oppenheimer, C., Pyle, D.M., Barclay, J. (Eds.), Volcanic Degassing, 213. Geological Society, London, Special Publication, pp. 219–230.